

Quantum $z = 2$ Lifshitz criticality in interacting topological chains

Ke Wang^{1,*}

¹*Kadanoff Center for Theoretical Physics, James Franck Institute,
Department of physics, University of Chicago, Chicago, IL 60637, USA*

(Dated: February 28, 2023)

We consider Lifshitz criticality (LC) with dynamical critical exponent $z = 2$ in the interacting topological chain. We report that interactions have crucial effects on Lifshitz criticality. We find that repulsive interaction derives the system to a conformal-invariant criticality and the low-energy excitations are gapless bosons. We also show that the attractive interaction stabilizes the $z = 2$ LC and excitations are almost free fermions carrying quadratic dispersion. The stability originates from the strong infrared quantum fluctuations compensating for the classical relevant perturbation. We perform numerical simulations to confirm the theoretical predictions and consider universal behaviors of quantum critical phases. The work paves the way to study interacting one-dimensional LCs and offers insights into low-dimensional quantum criticality.

Introduction. Strong infrared (IR) fluctuations play an important role in low-dimensional field theories. In classical two-dimensional (2D) field theories with continuous symmetries, emerging logarithmic IR divergences destroy the long-range order^{1,2} and results in the absence of spontaneous symmetry breaking^{3,4}. For quantum one-dimensional (1D) fermions, similar logarithmic divergences in loop diagrams destabilize single quasi-particles and lead to the breakdown of Fermi Liquids^{5,6}. The low-energy excitations become bosonic⁷ upon a weak interaction turned on. This is the celebrated Luttinger Liquid (LL) theory^{8–10}. Non-Fermi liquids in two-dimension remain as a puzzle due to strong IR fluctuations^{11–13}.

A large class of quantum criticality (QC) is described by relativistic conformal field theories^{14–17} (CFTs). In this context, there are many theoretical successes, e.g., operator product expansions¹⁸ and bosonizations¹⁹. However, there exists QC breaking relativistic conformal symmetry, e.g. Lifshitz criticalities (LCs)²⁰ and non-relativistic CFT in unitary Fermi gas^{21,22}. LCs are characterized by non-unit dynamical critical exponents, $z \neq 1$. They emerge in condensed matter models, e.g., topological chains²³ and Rydberg atoms²⁴. Unlike $z = 1$ CFTs, quantum statistics are important for LCs^{25,26},

Interactions are essential to LCs. At a system with a finite-size L , the fundamental scale for kinetic energy is $K \sim t/L^z$. The contact interaction has the scale $V \sim u_0/L$. Here t and u_0 are two coefficients to ensure the energy dimension. When $z > 1$ and $u_0 \neq 0$, $V/K \rightarrow \infty$ in the thermodynamic limit. Another infinity comes from quantum corrections. Consider the fermions with the dispersion, $\epsilon_{\pm}(k) = \pm t|k|^z$. The ground state is described by the Dirac Sea with all negative energy modes filled. Vacuum polarization from the creation of virtual particle-hole pairs introduces another infinity at zero energy limit. Two infinities make interacting LCs highly non-trivial. A fundamental question arises: what is the low-energy field theory of interacting LCs?

In this letter, we find the low-energy description of the interacting $z = 2$ LCs in both continuum theory and lattice models. When the interaction u is repulsive, the system flows to another universality class with

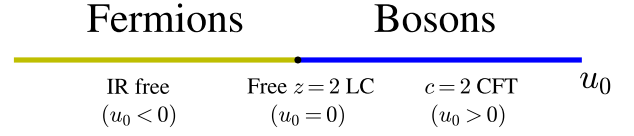


FIG. 1. (Color Online) Asymmetric property respective to the sign of interaction u (coupling constant). The spectrum is always gapless. (1). At $u < 0$, excitations are fermions and the coupling constant u flows to zero at IR limit. (2). At $u > 0$, the system flows to other universality class. Excitations are bosons and the low-energy theory is $c = 2$ CFT.

the dynamical critical exponent $z = 1$. The underlying field is bosonic and excitations are particle-hole collective modes. When the interaction is attractive, the system would not flow to other universality classes and remain at the $z = 2$ LC. The field is fermionic and the dispersion is quadratic. The interaction may slightly renormalize the curvature of dispersion. The peculiar property at the attractive region is contrasted with the instability of fermions in one-dimensional LL theory. The asymmetric property for $u_0 > 0$ v.s. $u_0 < 0$ is summarized in Fig. 1. Below we start with a simple discussion of lattice models and continuous field theories.

Model and Perturbative theory. The non-interacting $z = 2$ LC emerges from a slightly generalized Su–Schrieffer–Heeger (SSH) model²⁷,

$$H = \sum_{i=1}^L \sum_{l=0,1,2} \left(t_l \hat{c}_{i-l,A}^\dagger \hat{c}_{i,B} + h.c. \right) + u_0 \hat{n}_{i,A} \hat{n}_{i,B}. \quad (1)$$

Here $\hat{c}_{i,A/B}^\dagger$ is two-species fermion operator, L is the linear size of lattice and $\hat{n}_{i,A/B} = \hat{c}_{i,A/B}^\dagger \hat{c}_{i,A/B}$ is the particle number operator. t_l with $l = 1, 2, 3$ are three hopping parameters and u_0 is the interaction strength. The non-interacting $z = 2$ LC emerges at $t_0 = t_2 = t_1/2$. The low-energy effective theory of Eq. 1 around this point

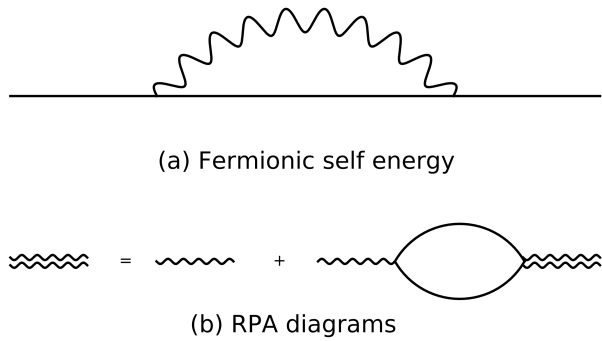


FIG. 2. (Color Online) Two perturbative Feynman diagrams. (a) The fermionic self-energy. The solid line is the free fermion propagator and the wavy line is the electronic interaction. (b) RPA diagrams. The double wavy represents the interaction renormalized by loop diagrams.

may be represented by the spectral basis,

$$\hat{H}_{\text{low-energy}} = \int dx \sum_{s=\pm} s \hat{\psi}_s^\dagger(x) (-i\partial_x)^2 \hat{\psi}_s(x) + u_0 \int dx \hat{\psi}_+^\dagger(x) \hat{\psi}_-^\dagger(x) \hat{\psi}_-(x) \hat{\psi}_+(x). \quad (2)$$

Here $\hat{\psi}_s^\dagger(x)$ is the field operator in the continuous space, $s = \pm$ are two spectral branches and t_0 (bandwidth) is set to be a unit. The non-interacting Feynman propagator is given by

$$G_s(k, \omega) = \frac{1}{\omega - sk^2 + i\delta \cdot \text{sign}(s)}, \quad s = \pm. \quad (3)$$

Here $\text{sign}(s)$ is the sign of s , denoting the particle/hole excitation, and $\delta = 0^+$. Since virtual particle-hole pairs renormalize quasi-particle and electronic interaction, we consider the polarization operator (PO). The definition is $\Pi_{s,s'}(q, \omega) = -i(2\pi)^{-2} \int dk d\omega' G_s(k, \omega') G_{s'}(k-q, \omega' - \omega)$. After the integral, it is given by

$$\Pi_{s,s'}(q, \omega) = \frac{1}{4} \frac{|s - s'|}{\sqrt{-2s\omega + q^2}}. \quad (4)$$

There emerges an algebraic singularity $\Pi(q, 0) \sim 1/q$, which is due to $z = 2$ dynamical critical exponent. $\Pi(q, \omega)$ becomes imaginary when $s\omega > q^2/2$, indicating that quasi-particles decay into particle-hole continuum. Inserting the one-loop diagram to Fig. 2a, one may obtain the self-energy correction. For particle-like fermions, the correction reads $\Sigma_+(k, \omega) \simeq -iu_0^2(2\pi)^{-2} \int dv dq G_-(k - q, \omega - \nu) \Pi_{+-}(q, \nu)$. After the integral, we find the imaginary part of Σ_+ ,

$$\text{Im}\Sigma_+(k=0, \omega) = \frac{u_0^2}{2} \left(\ln \frac{\Lambda}{\sqrt{|\omega|}} - (\sqrt{2\omega})^{-1} \frac{\Lambda}{2\pi} \Theta(\omega) \right) \quad (5)$$

Here Λ is the UV cut-off of the low-energy theory and Θ is the step function. One may conclude that the divergent $\text{Im}\Sigma(k=0, \omega \rightarrow 0^+)$ leads to a vanishing

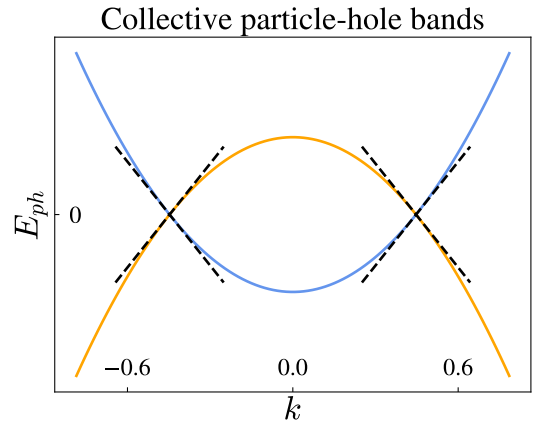


FIG. 3. (Color Online) Energy of collective modes at $u_0 = 0.1$. They are obtained from Eq. 6. Two bands cross each other at two points in the momentum space, $k = \pm\sqrt{2u_0}$. Near the crossing points, the dispersion becomes linear. Thus the low energy field theory is described by two copies of Luttinger liquids.

lifetime of quasi-particles, thus destabilizing fermions. The analysis does not tell the complete story, since u_0 should depend on Λ instead of being a simple constant. To obtain $u_0(\Lambda)$, one might perform momentum-shell renormalization and find the running coupling. Typically we are interested in the IR theory, and one should lower Λ to zero to see the fate of Eq. 5. This aspect will be discussed in the next section. The spectrum of particle-hole collective modes can be obtained by RPAs in Fig 2b. In LL theory, this method gives the same dispersion as the one obtained from the bosonization. RPA diagrams renormalize the bare Green function in Eq. 3 and the involved effective interaction is given by $u_s(q, \omega) \equiv u_0/(1 - u_0\Pi_{s,-s}(q, \omega))$, $s = \pm$. The spectrum of particle-hole collective excitations can be extracted by the poles of the effective interaction $u_s(q, \omega)$. Poles only exist within repulsive interactions and collective excitations have the spectrum,

$$E_s(q) = s(q^2/2 - u_0), \quad s = \pm, \quad (6)$$

when $u_0 > 0$. The spectrum of collective excitations is plotted in Fig. 3. Two bosonic bands intersect with each other at $q = \pm\sqrt{2u_0}$. Thus the system at $u_0 > 0$ is gapless and the low energy physics is described as two copies of Luttinger Liquids, namely $c = 2$.

Renormalization group. The bare Hamiltonian presented in Eq. 1 only assumes a constant u at a given energy scale. To track the coupling u at different energy scales, one may perform the momentum-shell renormalization of the bare action S . The method consists of iteratively lowering the energy scale Λ and obtaining the effective action with a lower energy scale. At each step of renormalization, new scattering events may be generated in the effective action. This leads to the renormalization group equation (RGE) of the coupling constant u .

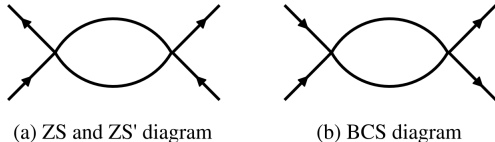


FIG. 4. (Color Online) Three diagrams renormalize the coupling function $u(k_4, k_3; k_2, k_1)$. (a) ZS or ZS' diagrams. The two diagrams share the same topology. But the momentum transfer at the vertex is different, $k_1 - k_3$ for ZS and $k_1 - k_4$ for ZS'. (b) BCS diagram. Momentum transfer at the vertex is $k_1 + k_2$.

We start from the corresponding bare action in the Euclidean space-time given by $S = S_0 + S_{\text{int}}$. The non-interacting action reads

$$S_0 = \sum_{s=\pm} \int \frac{dkd\omega}{(2\pi)^2} \bar{\psi}_s(\omega k)(i\omega - sk^2)\psi_s(\omega k), \quad (7)$$

and the interaction is written by a conventional symmetric potential,

$$S_{\text{int}} = \frac{1}{2!2!} \prod_{i=1,2,3,4} \int \frac{dk_i d\omega_i}{(2\pi)^2} u_{s_4 s_3 s_2 s_1} 2\pi \delta_k \cdot 2\pi \delta_\omega \\ \times \bar{\psi}_{s_4}(\omega_4 k_4) \bar{\psi}_{s_3}(\omega_3 k_3) \psi_{s_2}(\omega_2 k_2) \psi_{s_1}(\omega_1 k_1). \quad (8)$$

Here $\psi, \bar{\psi}$ is the Grassmannian variable and δ_k represents $\delta(k_4 + k_3 - k_2 - k_1)$. The potential is u_0 if $\{s_4 s_3 s_2 s_1\} = \{- - + +\}$ and 0 otherwise.

The canonical dimension of the fermion field is $5/2$. Therefore the coupling constant u is relevant, regardless of u being attractive or repulsive. This analysis from the classical scaling dimension is not enough for $z = 2$ LCs. Quantum corrections are not sub-leading due to their strong fluctuations near zero energy. In fact, when the coupling constant u is negative, it is indeed irrelevant perturbations.

Loop corrections emerge when one integrates higher energy modes and obtains the effective action for lower energy modes. At the second order approximation, three types of diagrams are important, plotted in Fig. 4 and called zero sound (ZS), zero sound' (ZS'), and BCS diagrams. The ZS/ZS' diagrams consider particle-hole channels and may indicate charge-density-wave (CDW) instability. The BCS diagram is from the particle-particle channel and gives the superconductor instability of the Fermi surface. For $z = 2$ LC, the creation of virtual particle-hole pairs is essential to the renormalization of interactions. At zero temperature, scatterings via particle-particle channels are absent. Thus the ZS/ZS' diagrams are the main contribution to the running coupling,

$$\Lambda \frac{du}{d\Lambda} = u + \frac{u^2}{2\pi\Lambda}. \quad (9)$$

Here Λ is the UV cut-off. Note that the second term depends on Λ explicitly. This is reminiscent of strong

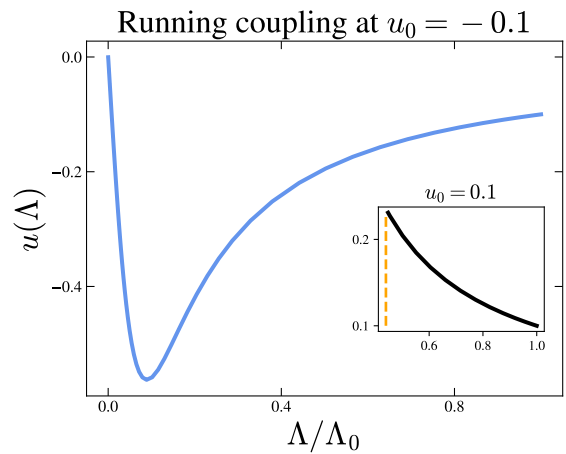


FIG. 5. (Color Online) Running coupling constant $u(\Lambda)$. The main plot is the solution to Eq. 9 with the initial condition $u_0 \equiv u(\Lambda_0) = -0.1$. The coupling would finally converge to zero when $\Lambda \rightarrow 0$. The inset is the solution with the initial condition $u_0 = 0.1$. The dashed line locates the coupling at $\Lambda = \sqrt{2u_0}$.

zero energy fluctuations, sharing the same origin of IR divergence in Eq. 4. We emphasize that this term *cannot* neglected although it is indeed zero at the limit $\Lambda \rightarrow \infty$.

The weight of quantum corrections in the running coupling becomes large when the cut-off runs to the IR regime. Consider such a scenario. The coupling constant is a small negative value u_0 at some finite cut-off Λ_0 s.t. $|u_0| \ll \Lambda_0$. With no doubt, quantum corrections are weak at the beginning and $|u_0|$ becomes larger since it is the "relevant" perturbation. The story remains true until Λ runs below $u(\Lambda)$. The crossing $\Lambda \sim u(\Lambda)$ must happen at some point Λ_c where the r.h.s of Eq. 9 changes the sign. Quantum corrections become dominating in the regime $\Lambda < \Lambda_c$ and $|u(\Lambda)|$ become smaller. Finally, the coupling vanishes when Λ approaches zero, with the universal asymptotics $u(\Lambda) \simeq -2\pi\Lambda$ (independent of initial conditions). The running coupling is solved numerically and plotted in Fig. 5.

We have argued that the negative coupling is irrelevant. But the fate of fermion quasi-particles is still unclear, since the zero energy divergence exists in Eq. 5. To answer the question, we consider the scenario where the UV cut-off Λ is lowered to be comparable with $\sim 1/\sqrt{L}$. The low energy excitation in $z = 2$ LC has the characteristic scale $\sim 1/L^2$. Therefore the inverse of quasi-particles lifetime scales as $\sim 1/\sqrt{L} - (\ln L)/L$. In the thermodynamic limit (or when the excitation energy approaches the Fermi point), the lifetime becomes infinite. This is nothing but the feature of Fermi Liquids theory.

RG analysis at the positive coupling shows that the interaction is a relevant perturbation since u flows $+$ in the limit $\Lambda \rightarrow 0$. But it cannot give the right description of new fixed points. A natural expectation is that the system might develop a charge-density-wave for A/B

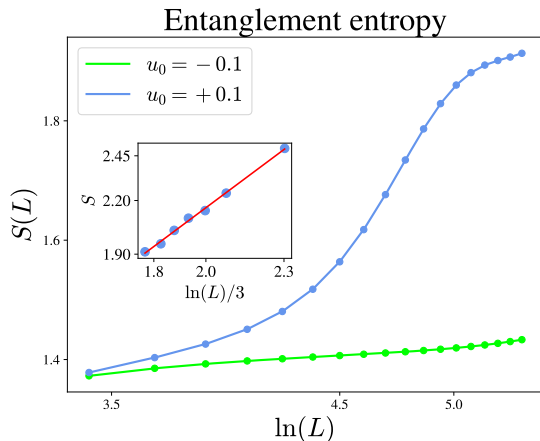


FIG. 6. (Color Online) Results of Entanglement entropy $S(L)$ at $u_0 = \pm 0.1$. Length varies from $L = 30$ to 200 . The $S(L)$ exhibits sharply different behaviors for positive/negative couplings. Entropy climbs quickly at $u_0 > 0$ while remaining almost constant at $u_0 < 0$. The inset plots the entropy at $u_0 = 0.1$ with $L \geq 200$. The linear fit (red line) is performed for entropy versus $1/3 \ln L$ when $200 \leq L \leq 510$. There exist weak oscillations of entropy around this linear line. The entropy at a large value $L = 1000$ is plotted to show the validity of the linear fit. The slope is found to be close to 1, indicating that the central charge is 2.

sublattice and the excitations are gapped. But we have seen from the RPA calculations that the system at the positive coupling is still gapless. More specifically, the gap is closed at the momentum scale $k \sim \sqrt{2u_0}$. This means that the cut-off cannot run to zero if one wants to obtain the true low-energy theory. In fact, by linearizing the spectrum in Fig. 3, one can see that the new fixed point is described by two copies of Luttinger liquids.

DMRG numerics. In this section, we use DMRG from ITensor²⁸ to simulate the lattice model in Eq. 1. We fix model parameters to $t_0 = t_2 = 1$ and $t_1 = 2$. The coupling constant u_0 is picked to be either $+0.1$ or -0.1 . The truncation error cutoff is taken to be 10^{-10} . We keep running sweeps until $E_i - E_{i-1} < 10^{-11}$ and $S_i - S_{i-1} < 10^{-8}$. Here E_i and S_i are the energy and entropy of the ground state at i -th sweep.

Predicted asymmetric many-body properties in Fig. 1 can be observed in the entanglement entropy of the ground state. Here we present the results of weak interactions in Fig. 6. At $u_0 = 0.1$, the entropy climbs quickly and deviates from behaviors of $z = 2$ LC, indicating a phase transition. At larger L , a clear CFT characteristic emerges. We also find that the central charge of the theory is $c = 2$, which is plotted in the inset of Fig. 6. This confirms predictions from Fig. 3. At $u_0 = -0.1$, the entropy remains almost constant, which is a fundamental feature of $z = 2$ LC. To confirm the dynamical critical exponent $z = 2$, we calculate the energy difference at $u_0 = -0.1$,

$$\Delta E = E_1(L) - E_0(L). \quad (10)$$

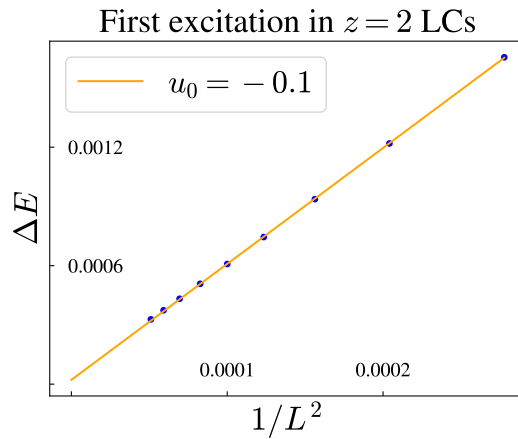


FIG. 7. (Color Online) Excitation energy v.s. system size L . The system size varies from 60 to 140 . The orange line is the linear fit. The linear coefficient is found to be $5.8(7)$. Compared to the slope $6.8(8)$ obtained from the free theory, the effective band curvature t becomes $0.8(5)$.

Here $E_1(L)$ is the energy of the first excitation and $E_0(L)$ is the energy of the ground state. We find that $\Delta E(L)$ is a linear function of $1/L^2$. See Fig. 7.

Ground state energy of $z = 2$ LCs contains a universal amplitude, as described in Ref. 26. More specifically, one may write the ground state energy as

$$E_0(L) = L\epsilon + b - m \frac{J}{L^2} + O(L^{-3}). \quad (11)$$

Here m is the non-universal curvature of the quadratic band and J is the universal amplitude. In several free theories, e.g., SSH models and Majorana chains, J is numerically given by $J \simeq 0.886$. When $u_0 = -0.1$, the J is numerically found to be $0.8(8)$. Thus, from the universal finite-size amplitude, we further confirm that the low-energy description of the lattice model at $u_0 = -0.1$ is the $z = 2$ LCs.

Conclusions. Interactions effects are essential to the $z = 2$ LC. We find that a positive interaction drives the $z = 2$ LC to $c = 2$ CFT. Fermion excitation in $z = 2$ LC is unstable to a very small positive interaction and particle-hole collective modes become low-energy excitations. We also show that the $z = 2$ LC is stable to a negative interaction. An interesting relevant-irrelevant RG scheme is used to explain this intriguing phenomenon.

Phase diagrams versus the interaction and other relevant perturbations (velocity, mass) are left for future study. It remains an interesting question to see whether the $z = 2$ LC could be a critical phase in the two-dimensional phase diagram (e.g. versus u and t_0). Another interesting question is whether one can tune model parameters to create $z = 2$ LC where low-energy excitations are bosonic. Long-range interactions and dynamical gauge couplings are not considered in the present work, remaining open questions.

Acknowledgment. K. W. thanks insightful discussions with D. T. Son, L. Delacretaz, K. Levin, Z. Q. Wang, X. C. Wu, and U. Mehta about RG and general issues. K. W. thanks very helpful discussions with Jin Zhang on

DMRG. K. W. also thanks early stimulating discussions with T. Sedrakyan, W. Witczak-Krempa, A. Klein, Y. H. Zhang, and A. Hui. K. W. is supported, in part, by Kadanoff Center.

-
- * kewang07@uchicago.edu
- ¹ N. D. Mermin and H. Wagner, “Absence of ferromagnetism or antiferromagnetism in one- or two-dimensional isotropic heisenberg models,” *Phys. Rev. Lett.* **17**, 1133 (1966).
 - ² V. L. Berezinsky, “Destruction of long range order in one-dimensional and two-dimensional systems having a continuous symmetry group. I. Classical systems,” *Sov. Phys. JETP* **32**, 493–500 (1971).
 - ³ S. Coleman, “There are no goldstone bosons in two dimensions,” *Communications in Mathematical Physics* **31**, 259 (1973).
 - ⁴ J. M. Kosterlitz and D. J. Thouless, “Ordering, metastability and phase transitions in two-dimensional systems,” *Journal of Physics C: Solid State Physics* **6**, 1181 (1973).
 - ⁵ A. A. Abrikosov, I. Dzyaloshinskii, L. P. Gorkov, and Richard A. Silverman, *Methods of quantum field theory in statistical physics* (Dover, New York, NY, 1975).
 - ⁶ T. Giamarchi, *Quantum physics in one dimension*, International series of monographs on physics (Clarendon Press, Oxford, 2004).
 - ⁷ S. Tomonaga, “Remarks on Bloch’s Method of Sound Waves applied to Many-Fermion Problems,” *Progress of Theoretical Physics* **5**, 544 (1950).
 - ⁸ J. M. Luttinger, “An exactly soluble model of a many-fermion system,” *Journal of Mathematical Physics* **4**, 1154 (1963).
 - ⁹ F. D. M. Haldane, “Luttinger liquid theory of one-dimensional quantum fluids. i. properties of the luttinger model and their extension to the general 1d interacting spinless fermi gas,” *Journal of Physics C: Solid State Physics* **14**, 2585 (1981).
 - ¹⁰ A. Imambekov, T. L. Schmidt, and L. I. Glazman, “One-dimensional quantum liquids: Beyond the luttinger liquid paradigm,” *Rev. Mod. Phys.* **84**, 1253–1306 (2012).
 - ¹¹ Sung-Sik Lee, “Low-energy effective theory of fermi surface coupled with U(1) gauge field in 2 + 1 dimensions,” *Phys. Rev. B* **80**, 165102 (2009).
 - ¹² F. Borges, A. Borissov, A. Singh, A. Schliefl, and Sung-Sik Lee, “Field-theoretic functional renormalization group formalism for non-fermi liquids and its application to the antiferromagnetic quantum critical metal in two dimensions,” (2022).
 - ¹³ M. A. Metlitski and S. Sachdev, “Quantum phase transitions of metals in two spatial dimensions. i. ising-nematic order,” *Phys. Rev. B* **82**, 075127 (2010).
 - ¹⁴ A. A. Belavin, A. M. Polyakov, and A. B. Zamolodchikov, “Infinite conformal symmetry in two-dimensional quantum field theory,” *Nuclear Physics B* **241**, 333 (1984).
 - ¹⁵ I. Affleck, “Universal term in the free energy at a critical point and the conformal anomaly,” *Phys. Rev. Lett.* **56**, 746 (1986).
 - ¹⁶ H. W. J. Blöte, John L. Cardy, and M. P. Nightingale, “Conformal invariance, the central charge, and universal finite-size amplitudes at criticality,” *Phys. Rev. Lett.* **56**, 742 (1986).
 - ¹⁷ P. Di Francesco, P. Mathieu, and D. Senechal, *Conformal Field Theory*, Graduate Texts in Contemporary Physics (Springer-Verlag, New York, 1997).
 - ¹⁸ K. G. Wilson, “Non-lagrangian models of current algebra,” *Phys. Rev.* **179**, 1499 (1969).
 - ¹⁹ D. C. Mattis and E. H. Lieb, “Exact solution of a many-fermion system and its associated boson field,” *Journal of Mathematical Physics* **6**, 304 (1965).
 - ²⁰ P. Hořava, “Quantum gravity at a lifshitz point,” *Phys. Rev. D* **79**, 084008 (2009).
 - ²¹ Y. Nishida and D. T. Son, “Nonrelativistic conformal field theories,” *Phys. Rev. D* **76**, 086004 (2007).
 - ²² S. Golkar and Dam T. Son, “Operator product expansion and conservation laws in non-relativistic conformal field theories,” *Journal of High Energy Physics* **2014**, 63 (2014).
 - ²³ R. Verresen, N. G. Jones, and F. Pollmann, “Topology and edge modes in quantum critical chains,” *Phys. Rev. Lett.* **120**, 057001 (2018).
 - ²⁴ N. Chepiga and F. Mila, “Lifshitz point at commensurate melting of chains of rydberg atoms,” *Phys. Rev. Research* **3**, 023049 (2021).
 - ²⁵ C. Boudreault, C. Berthiere, and W. Witczak-Krempa, “Entanglement and separability in continuum rokhsarkivelson states,” (2021).
 - ²⁶ K. Wang and T. A. Sedrakyan, “Universal finite-size amplitude and anomalous entanglement entropy of $z = 2$ quantum Lifshitz criticalities in topological chains,” *SciPost Phys.* **12**, 134 (2022).
 - ²⁷ W. P. Su, J. R. Schrieffer, and A. J. Heeger, “Solitons in polyacetylene,” *Phys. Rev. Lett.* **42**, 1698 (1979).
 - ²⁸ M. Fishman, S. R. White, and E. M. Stoudenmire, “The ITensor Software Library for Tensor Network Calculations,” *SciPost Phys. Codebases*, 4 (2022).

Supplemental Material: Quantum $z = 2$ Lifshitz criticality in interacting topological chains

I. PERTURBATIVE CALCULATIONS

A. Derivation of Polarization operator

We start with the definition of the polarization operator,

$$\Pi_{s,s'}(q, \omega) = -i \int \frac{dk}{2\pi} \frac{d\omega'}{2\pi} G_0^s(k, \omega') G_0^{s'}(k - q, \omega' - \omega). \quad (\text{S1})$$

Insert the expression of the propagators,

$$\Pi_{s,s'}(q, \omega) = -i \int \frac{dk}{2\pi} \frac{d\omega'}{2\pi} \frac{1}{\omega' - s\epsilon(k) + i\delta \text{sgn}(\omega')} \frac{1}{\omega' - \omega - s'\epsilon(k - q) + i\delta \text{sgn}(\omega' - \omega)}. \quad (\text{S2})$$

Note that in the integral, the effect of $\text{sgn}(\omega)$ is the same as the s . Therefore we define

$$f_{s,s'}(k, q) = \int_{-\infty}^{\infty} \frac{d\omega'}{2\pi} \frac{1}{\omega' - s\epsilon(k) + is\delta} \frac{1}{\omega' - \omega - s'\epsilon(k - q) + is'\delta} \quad (\text{S3})$$

Now it is purely about applying the residue theorem in the complex analysis. That gives

$$\begin{aligned} \text{if } s = s', \quad f_{s,s'}(k, q) &= 0 \\ \text{if } s = -s', \quad f_{s,s'}(k, q) &= is \frac{1}{-\omega + s\epsilon(k) + s\epsilon(k - q) - is\delta} = -i \frac{1}{s\omega - \epsilon(k) - \epsilon(k - q) + i\delta} \end{aligned} \quad (\text{S4})$$

Thus one reaches the integral expression,

$$\Pi_{s,s'}(q, \omega) = -(\sigma_x^{s,s'}) \int \frac{dk}{2\pi} \frac{1}{s\omega - \epsilon(k) - \epsilon(k - q) + i\delta}. \quad (\text{S5})$$

One may make use of energy expression and redefine the integral variable $k = k - q/2$,

$$\Pi_{s,-s}(q, \omega) = - \int_{-\infty}^{+\infty} \frac{dk}{2\pi} \frac{1}{s\omega - 2(k - q/2)^2 - q^2/2 + i\delta} = \int_{-\infty}^{+\infty} \frac{dk}{4\pi} \frac{1}{k^2 + q^2/4 - s\omega/2 - i\delta}.$$

Below we give an analysis based on the sign of $q^2/4 - s\omega/2$.

- If $q^2/4 - s\omega/2 > 0$, δ is not important and can be taken as zero. One may need the equation below,

$$\int_{-\infty}^{+\infty} \frac{dz}{2\pi} \frac{1}{z^2 + a^2} = \int_{-\infty}^{+\infty} \frac{dz}{2\pi} \frac{1}{(z + ia)(z - ia)} \quad (\text{S6})$$

Deforming the contour to the upper arc, one finds

$$\Pi_{s,-s}(q, \omega) = \frac{1}{2\sqrt{-2s\omega + q^2}}, \quad \text{if } q^2/4 + s\omega/2 > 0 \quad (\text{S7})$$

- If $q^2/4 - s\omega/2 < 0$, the PO may be rewritten as

$$\Pi_{s,-s}(q, \omega) = \int_{-\infty}^{\infty} \frac{dk}{4\pi} \frac{1}{k^2 - a^2 - i\delta} = -\frac{i}{4} \frac{1}{\sqrt{|-s\omega/2 + q^2/4|}} \quad (\text{S8})$$

where $a^2 = |q^2/4 - s\omega/2|$

Therefore, one can reach a simple expression,

$$\Pi_{s,s'}(q, \omega) = \frac{1}{4} \frac{|s - s'|}{\sqrt{-2s\omega + q^2}}. \quad (\text{S9})$$

This is Eq. 4 in the main text.

B. Derivation of Self-energy

Correction to the green function may be obtained by inserting the self-energy,

$$\delta G_+(k, \omega) = G_+(k, \omega) \Sigma_+(k, \omega) G_+(k, \omega). \quad (\text{S10})$$

At the one-loop level, the self-energy is approximated by

$$\Sigma_+(k, \omega) \simeq -iu_0^2 \int \frac{d\nu}{2\pi} \int \frac{dq}{2\pi} G_-(k-q, \omega-\nu) \Pi_{+,-}(q, \nu) \quad (\text{S11})$$

Now we trace the imaginary part of Σ_+ .

$$\text{Im}\Sigma_+(k, \omega) \equiv F_1 + F_2; \quad (\text{S12})$$

where $F_{1/2}$ involves the product of two imaginary/real parts of G and Π ,

$$F_1 = \int \frac{d\nu}{2\pi} \int \frac{dq}{2\pi} \text{Im}G_-(k-q, \omega-\nu) \text{Im}\Pi_{+,-}(q, \nu), \quad (\text{S13})$$

$$F_2 = - \int \frac{d\nu}{2\pi} \int \frac{dq}{2\pi} \text{Re}G_-(k-q, \omega-\nu) \text{Re}\Pi_{+,-}(q, \nu). \quad (\text{S14})$$

Below we evaluate two integrals of F_1 and F_2 .

Evaluation of F_1 . Note that $\text{Im}G_-(k-q, \omega-\nu) = \alpha\pi\delta(\omega-\nu+\epsilon_{k-q})$ and

$$\text{Im}\Pi_{+,-}(q, \nu) = \frac{1}{2\sqrt{2}u\sqrt{\nu-q^2/2}} \Theta(\nu-q^2/2) \quad (\text{S15})$$

Then one may obtain

$$F_1 = \frac{u_0^2}{2\sqrt{2}} \int \frac{dq}{2\pi} \int \frac{d\nu}{2\pi} \pi\delta(\omega-\nu+\epsilon_{k-q}) \frac{1}{\sqrt{\nu-q^2/2}} \Theta(\nu-q^2/2). \quad (\text{S16})$$

The delta function can be integrated out firstly,

$$F_1 = \frac{u_0^2}{4\sqrt{2}} \int \frac{dq}{2\pi} \frac{1}{\sqrt{\omega+(k-q)^2-q^2/2}} \Theta(\omega+(k-q)^2-q^2/2)$$

Use the identity below

$$(k-q)^2 - \frac{q^2}{2} = \frac{1}{2}(q-2k)^2 - k^2 \quad (\text{S17})$$

Then J_+ can be expressed as

$$J_+ = \frac{u_0^2}{4\sqrt{2}} \int \frac{dq}{2\pi} \frac{1}{\sqrt{\omega+q^2/2-k^2}} \Theta(\omega+q^2/2-k^2) \quad (\text{S18})$$

Now consider two different scenarios based on the sign of $\omega/u - k^2$.

(a), $\omega/u - k^2 \geq 0$. In this case, one may call $Q^2 = 2(\omega/u - k^2)$. Then the integral becomes

$$J_+ = \frac{u_0^2}{2} \int_0^\infty \frac{dq}{2\pi} \frac{1}{\sqrt{q^2+Q^2}} = \frac{u_0^2}{2} \ln \frac{\Lambda + \sqrt{\Lambda^2 + Q^2}}{Q}, \quad Q \geq 0 \quad (\text{S19})$$

where Λ is the UV cutoff. We may claim the result below

$$J_+ \simeq \frac{u_0^2}{2} \ln \frac{\Lambda}{\sqrt{\omega/u - k^2}} \quad (\text{S20})$$

One may observe a blow-up at the on-shell condition $\omega = uk^2$. It is traced back to an infrared divergence in the integral. This could be avoided if we have $f(q) \simeq q^z$ with $z \geq 1/2$. Even in the off-shell case, J_+ is still logarithmically large.

(b). $\omega/u - k^2 \leq 0$. In this case, one writes $Q^2 = 2(k^2 - \omega/u)$. The integral becomes

$$J_+ = \frac{u_0^2}{2} \int_Q^\infty \frac{dq}{2\pi} \frac{1}{\sqrt{q^2 - Q^2}} = \frac{u_0^2}{2} \cosh^{-1} \left(\frac{\Lambda}{Q} \right) \simeq \frac{u_0^2}{2} \ln \frac{\Lambda}{k^2 - \omega/u} \quad (\text{S21})$$

As a summary of J_+ , we find the expression valid for arbitrary $\omega/u - k^2$,

$$J_+ = J_+ \simeq \frac{u_0^2}{2} \ln \frac{\Lambda}{|\omega/u - k^2|}. \quad (\text{S22})$$

Evaluation of F_2 . In the previous calculation, we only focus on the imaginary part. The real part of polarization becomes

$$\text{Re}\Pi_{+-}(q, \omega) = \frac{1}{2\sqrt{2}\sqrt{-\omega/u + q^2/2}} \Theta(-\omega/u + q^2/2) \quad (\text{S23})$$

The real part of the propagator carries the principal part (which simply means deleting the pole),

$$\text{Re}G_{-\alpha}(k, \omega) = P \frac{1}{\omega + \alpha uk^2/2}. \quad (\text{S24})$$

With the variable change $x = q^2/2 - \nu$, one may write the integral expression,

$$F_2 \simeq -u_0^2 \int \frac{dx}{2\pi} \int \frac{dq}{2\pi} P \frac{1}{\omega + x + k^2/2 - kq} \frac{1}{2\sqrt{2}\sqrt{x}} \Theta(x). \quad (\text{S25})$$

As the first step, we consider the integral over q ,

$$\int \frac{dq}{2\pi} P \frac{1}{\omega + x + k^2/2 - ukq} = \frac{1}{k} \int \frac{dq}{2\pi} P \frac{1}{\omega/k + x/k + k/2 - q}. \quad (\text{S26})$$

Denoting $Y = \omega/uk + x/k + k/2$, one may write Eq. S26 as

$$\frac{1}{uk} \int \frac{dq}{2\pi} P \frac{1}{Y - q} = -\frac{1}{uk} \left(\int_{-\Lambda}^{Y-\epsilon} + \int_{Y+\epsilon}^{\Lambda} \right) \frac{dq}{2\pi} \frac{1}{q - Y} \quad (\text{S27})$$

One may notice that, if $\Lambda/Y \rightarrow \infty$, the integral above vanishes. In the asymptotic limit $\Lambda/Y \gg 1$, Eq. S26 can be reduced to be,

$$-\frac{1}{uk} \ln \frac{\Lambda - Y}{\Lambda + Y} = -\frac{1}{uk} \ln \left(1 - \frac{2Y}{\Lambda + Y} \right) \simeq \frac{1}{uk} \frac{2Y}{\Lambda}. \quad (\text{S28})$$

Thus in this limit, $\text{Im}\Sigma_\alpha(k, \omega)$ is small. Now we consider the opposite limit $k = 0$, i.e., Y goes to infinity. The integral expression of F_2 is simple,

$$F_2 \simeq -u_0^2 \int \frac{dx}{2\pi} \int \frac{dq}{2\pi} P \frac{1}{\omega + x} \frac{1}{2\sqrt{2}\sqrt{x}} \Theta(x). \quad (\text{S29})$$

The variable q is free and the integral of it immediately gives,

$$F_2 \simeq -u_0^2 \frac{\Lambda}{\pi} \int_0^\infty \frac{dx}{2\pi} P \frac{1}{\omega + x} \frac{1}{2\sqrt{2}\sqrt{x}}. \quad (\text{S30})$$

Now we replace the variable $x = z^2$,

$$F_2 = -u_0^2 \frac{\Lambda}{2\sqrt{2}\pi} \int_{-\infty}^\infty \frac{dz}{2\pi} \frac{1}{\omega + z^2}. \quad (\text{S31})$$

When $\omega > 0$, the integral above gives

$$F_2 = -u_0^2 \frac{\Lambda}{4\sqrt{2}\pi} \frac{1}{\sqrt{\omega}} \quad (\text{S32})$$

When $\omega < 0$, F_2 is zero. To check this, one may need to consider

$$F_2 \propto \int_0^\infty \frac{dz}{2\pi} P \frac{1}{-|\omega| + uz^2} = \left(\int_0^{\sqrt{|\omega|} - \delta} \frac{dz}{2\pi} + \int_{\sqrt{|\omega|} + \delta}^\infty \frac{dz}{2\pi} \right) \frac{1}{-|\omega| + z^2} \quad (\text{S33})$$

Recall that $\int \frac{dz}{z^2 - a^2} = \frac{1}{2a} \ln \frac{z-a}{z+a}$. Thus the integrals becomes $-\frac{1}{2\sqrt{|\omega|}} \ln \frac{\delta}{2\sqrt{\omega}} + \frac{1}{2\sqrt{|\omega|}} \ln \frac{\delta}{2\sqrt{\omega}} = 0$. Therefore one obtains the expression of F_2 ,

$$F_2 = -u_0^2 \frac{\Lambda}{4\sqrt{2\pi}} \frac{1}{\sqrt{|\omega|}} \Theta(\omega) \quad (\text{S34})$$

Combining F_1 and F_2 , one can obtain Eq. 5 in the main text.

II. RENORMALIZATION GROUP

In the momentum-shell method, the RG is implemented by: (1), integrating out the fast modes (2) obtaining the effective Lagrangian (3) Introduce the re-scaled parameters and field operators (which are used to keep Gaussian action invariant).

Now we have a bare theory defined by Lagrangian and action. Separate the field operator into slow and fast modes

$$\psi(k) = \psi_>(k) + \psi_<(k), \quad >: \Lambda/s < k < \Lambda, \quad <: 0 < k < \Lambda/s. \quad (\text{S35})$$

The operator $\psi_>(k)$ is defined by $\psi_>(k) = \psi(k)$ if $\Lambda/s < k < \Lambda$, otherwise zero. Similar definition for $\psi_<(k)$. Then the bare action/Lagrangian can be written as

$$Z = \int D[\psi_>] D[\psi_<] e^{S(\psi_>, \psi_<)}, \quad S(\psi_>, \psi_<) = S_0(\psi_>) + S_0(\psi_<) + S_{\text{int}}(\psi_>, \psi_<) \quad (\text{S36})$$

Effective action of $\psi_<$ can be obtained by integrating out the fast modes,

$$Z = \int D[\psi_<] e^{S_0(\psi_<)} \int D[\psi_>] e^{S_0(\psi_>)} e^{S_{\text{int}}(\psi_>, \psi_<)} = Z_> \int D[\psi_<] e^{S_0(\psi_<)} \langle e^{S_{\text{int}}(\psi_>, \psi_<)} \rangle_> \quad (\text{S37})$$

This equation determines the effective Lagrangian of $\psi_<$. The average of interacting exponential is performed for the Gaussian action of $\psi_>$. The technical part is about evaluating the perturbation of S_{int} , which follows from

$$\log \langle e^{S_{\text{int}}(\psi_>, \psi_<)} \rangle_> \simeq \langle S_{\text{int}} \rangle_> + \frac{\langle S_{\text{int}}^2 \rangle_> - \langle S_{\text{int}} \rangle_>^2}{2} + O(S_{\text{int}}^3) \quad (\text{S38})$$

The result is generally valid from cumulant expansion. Here I have hidden the dependence of S on the field operators. Then the effective Lagrangian/action can be obtained perturbatively,

$$S_{\text{eff}}(\psi_<) \simeq S_0(\psi_<) + \langle S_{\text{int}} \rangle_> + \frac{\langle S_{\text{int}}^2 \rangle_> - \langle S_{\text{int}} \rangle_>^2}{2} + \dots \quad (\text{S39})$$

Here I only preserve up to the second order. One can perform higher-order perturbation, which is fundamentally equivalent to plotting connected Feynman diagrams. Although the first/second orders are written separately, they may contribute to the same coupling constant. Similar behaviors may happen for higher perturbations. One shall be careful about arguing that high-order perturbations do not change results.

To study the RG flow of coupling constant in $S_{\text{eff}}(\psi_<)$, one has to introduce the new momentum/frequency and field operators,

$$k' = sk, \quad \omega' = s^z \omega, \quad \psi'(k') = s^{-(2z+1)/2} \psi_<(k) \quad (\text{S40})$$

Here k/ω is the old momentum/frequency (note that k only lies in the smaller momentum region $<$) and k'/ω' are new ones. Then perform change of variables in S_{eff} in Eq. S40. One would observe that the S_0 is invariant under this re-scale process (or more precisely the non-interacting parameter is invariant). Other coupling constants shall be also expressed in terms of this new set of variables/fields. Below we handle the theory perturbatively.

A. First order in interaction

The first-order perturbation involves the average,

$$\begin{aligned} \langle S_{\text{int}} \rangle_{0>} &= \frac{1}{2!2!} \prod_{i=1,2,3,4} \left[\int_{|k|<\Lambda} \frac{dk_i}{(2\pi)} \int_{-\infty}^{+\infty} \frac{d\omega_i}{2\pi} \right] u_{i_4 i_3 i_2 i_1} (4321) \langle \bar{\psi}_{i_4}(4) \bar{\psi}_{i_3}(3) \psi_{i_2}(2) \psi_{i_1}(1) \rangle_{0>} \\ &\times 2\pi \delta(k_4 + k_3 - k_2 - k_1) 2\pi \delta(\omega_4 + \omega_3 - \omega_2 - \omega_1) \end{aligned} \quad (\text{S41})$$

Express 4-point correlation into fast and slow modes,

$$\langle \bar{\psi}_{i_4} \bar{\psi}_{i_3} \psi_{i_2} \psi_{i_1} \rangle_{0>} = \langle (\bar{\psi}_{i_4,<} + \bar{\psi}_{i_4,>}) (\bar{\psi}_{i_3,<} + \bar{\psi}_{i_3,>}) (\psi_{i_2,<} + \psi_{i_2,>}) (\psi_{i_1,<} + \psi_{i_1,>}) \rangle_{0>} \quad (\text{S42})$$

One can expand the brackets. Non-zero contributions consist of three types: (1). 4 slow terms, namely, tree-level scaling. (2) 2 slow /2 fast terms. This part gives corrections to the Gaussian part. (3) 4 fast terms, giving a constant in effective action thus negligible.

- *Tree-level.* This level is nothing but performing power counting based on Eq. S40. This leads to

$$v'(4'3'2'1') = s^{-3(z+1)+2(2z+1)} v(4321) = s^{z-1} v(4321). \quad (\text{S43})$$

The first part is from the re-scale of variables while the second part is from field operators. If $z = 1$, it is marginal perturbation which is typical for Luttinger liquid. If $z = 2$, it becomes a relevant perturbation even at the classical level.

- *Correction to Gaussian action.* Here we consider the symmetric potential and take the constant potential. Via some simple combinatorics, one would see terms like

$$-4u_0 \bar{\psi}_{<,-} (4) \psi_{<,-} (3) \langle \bar{\psi}_{>,+} (2) \psi_{>,+} (1) \rangle - 4u_0 \bar{\psi}_{<,+} (4) \psi_{<,+} (3) \langle \bar{\psi}_{>,-} (2) \psi_{>,-} (1) \rangle. \quad (\text{S44})$$

Note 1 contains both momentum and frequency. But the notation is abused: in the previous calculation. The average here is simply the Gaussian type of integral with

$$\langle \bar{\psi}_{\alpha>}(\omega k) \psi_{\beta>}(\omega' k') \rangle = \frac{\delta_{\alpha\beta}}{i\omega - \alpha u k^2} 2\pi \delta(k - k') 2\pi \delta(\omega - \omega') \quad (\text{S45})$$

Thus, in Eq. S41, this delta function only preserves one integral in fast modes. The conservation of total momentum makes the momenta of two slow modes equal.

$$\langle S_{\text{int}} \rangle_{0>} = -u_0 \int_{|k| < \Lambda/s} \frac{dk}{(2\pi)} \int_{-\infty}^{+\infty} \frac{d\omega}{2\pi} \sum_{\alpha=\pm} \bar{\psi}_{<,\alpha}(k\omega) \psi_{<,\alpha}(k\omega) \int_{|k_1| > \Lambda/s} \frac{dk_1}{2\pi} \int \frac{d\omega_1}{2\pi} \frac{e^{i\epsilon 0^+}}{i\omega_1 + \alpha k_1^2}$$

The integral can be explicitly down, e.g.,

$$\int_{|k_1| > \Lambda/s} \frac{dk_1}{2\pi} \int \frac{d\omega_1}{2\pi} \frac{e^{i\epsilon 0^+}}{i\omega_1 + k_1^2} = \int_{\Lambda > |k_1| > \Lambda/s} \frac{dk_1}{2\pi} = \frac{\Lambda(1-s^{-1})}{\pi} \quad (\text{S46})$$

Thus the correction to the Gaussian action reads

$$\langle S_{\text{int}} \rangle_{0>} = -u_0 \int_{|k| < \Lambda/s} \frac{dk}{(2\pi)} \int_{-\infty}^{+\infty} \frac{d\omega}{2\pi} \sum_{\alpha=\pm} \bar{\psi}_{<,\alpha}(k\omega) \psi_{<,\alpha}(k\omega) \frac{\Lambda(1-s^{-1})}{\pi} \quad (\text{S47})$$

This correction is simply a constant shift to the theory. One can introduce such a counter-term back to the bare Lagrangian s.t. there is no induced RG flow on the Gaussian theory part.

B. Second-order in interaction

Second-order perturbation involves the term below,

$$u_{i_4 i_3 i_2 i_1} (4321) (\bar{\psi}_{i_4,<} + \bar{\psi}_{i_4,>}) (\bar{\psi}_{i_3,<} + \bar{\psi}_{i_3,>}) (\psi_{i_2,<} + \psi_{i_2,>}) (\psi_{i_1,<} + \psi_{i_1,>}) \\ \times u_{i'_4 i'_3 i'_2 i'_1} (4'3'2'1') (\bar{\psi}_{i'_4,<} + \bar{\psi}_{i'_4,>}) (\bar{\psi}_{i'_3,<} + \bar{\psi}_{i'_3,>}) (\psi_{i'_2,<} + \psi_{i'_2,>}) (\psi_{i'_1,<} + \psi_{i'_1,>}) \quad (\text{S48})$$

There are 2^8 terms. Since the average is done over the Gaussian distribution, one only needs to trace even terms.

- $8\psi_{>}/0\psi_{<}$. This term is purely giving constant contribution.
- $6\psi_{>}/2\psi_{<}$. Gives renormalization to the non-interacting part but in higher order in u_0 .

- $4\psi_>/4\psi_<$. This term renormalizes the quartic interaction.
- $2\psi_>/6\psi_<, 0\psi_>/8\psi_<$. These terms are indeed generated in the re-normalization process.

Corrections to the quartic term. To list all possible terms generating quartic corrections, one may enumerate all possible terms in some principle. Since two interaction potentials are involved, one may list terms from (1). Two come-in (creation) operators from one potential while two come-out (annihilation) operators arise from one potential. (2) One come-in is from one potential while the other come-in is from one potential. From this principle, there are only two types. To symmetrize the local potential in momentum space, the second type is classified into two types. To see how this happen, let us consider the short-hand representation below (which is used to analyze the expansion),

$$u(4321)\bar{\psi}(4)\bar{\psi}(3)\psi(2)\psi(1) \times u(8765)\bar{\psi}(8)\bar{\psi}(7)\psi(6)\psi(5). \quad (\text{S49})$$

Each field operator here contains both $>$ and $<$. Now consider one piece of contribution in Eq. S49

$$u(8765)u(4321)\bar{\psi}_>(4)\bar{\psi}_<(3)\psi_>(2)\psi_<(1)\bar{\psi}_>(8)\bar{\psi}_<(7)\psi_>(6)\psi_<(5). \quad (\text{S50})$$

Note that the average will be done on the $>$ components. Thus a simple re-arrangement leads to

$$-u(8765)u(4321)\bar{\psi}_<(3)\bar{\psi}_<(7)\psi_<(1)\psi_<(5)\langle\bar{\psi}_>(4)\psi_>(2)\bar{\psi}_>(8)\psi_>(6)\rangle \quad (\text{S51})$$

There is only one way to pair field operators in a connected way,

$$u(8765)u(4321)\bar{\psi}_<(3)\bar{\psi}_<(7)\psi_<(1)\psi_<(5)G(4)\delta(4,6)G(2)\delta(2,8) \quad (\text{S52})$$

Then taking integral and delta-function (momentum/energy conservations) into consideration, one finds that S_{int}^2 contains the contribution like

$$\delta(4+3-2-1)\bar{\psi}_<(4)\bar{\psi}_<(3)\psi_<(2)\psi_<(1)\int d5d6G(5)G(6)\delta(3+5-1-6)u(6452)u(5361)$$

In fact, exchanging the role of 1 and 2 leads to another form of expression,

$$-\delta(4+3-2-1)\bar{\psi}_<(4)\bar{\psi}_<(3)\psi_<(2)\psi_<(1)\int d5d6G(5)G(6)\delta(3+5-2-6)u(6451)u(5362)$$

This exchange seems to be trivial but important in obtaining a symmetric vertex correction. Since there are totally 2^4 terms in the second type contributing the same as Eq. S53, one may split them into so-called ZS and ZS' diagrams. To be consistent with the reference, we play some variable change and reach,

$$ZS = \bar{\psi}_<(4)\bar{\psi}_<(3)\psi_<(2)\psi_<(1)\int d5d6G(5)G(6)\delta(3+5-1-6)u(6351)u(4526) \quad (\text{S53})$$

$$ZS' = -\bar{\psi}_<(4)\bar{\psi}_<(3)\psi_<(2)\psi_<(1)\int d5d6G(5)G(6)\delta(3+5-2-6)u(6451)u(3526) \quad (\text{S54})$$

Note identity coefficient comes from $8/(2 \times 2! \times 2!) = 1$. Of course, the first type of contribution is the so-called BCS diagram. It contributes as

$$BCS = -\frac{1}{2}\bar{\psi}_<(4)\bar{\psi}_<(3)\psi_<(2)\psi_<(1)\int d5d6G(5)G(6)\delta(5+6-4-3)u(4365)u(6521)$$

The coefficient $1/2$ comes from $4/8$. Now we have symbolically represented one-loop level contributions. One would see that this is equivalent to the usual Feynman diagrams of four-point correlations. Now we consider the loop-correction to $u(+ - + -)$, i.e., $4 = +, 3 = -, 2 = +, 1 = -$.

- *ZS diagram.* From the specific potential condition, we demand that the sub-indices part satisfies

$$63 = 51 = 54 = 26 = \{+, -\}. \quad (\text{S55})$$

It is easy to see that this is impossible. Thus contribution from ZS diagram to this typical potential vanishes.

- *ZS' diagram.* From the specific potential condition, we demand that the sub-indices part satisfies

$$64 = 51 = 35 = 26 = \{+, -\}. \quad (\text{S56})$$

It is easy to conclude that $6 = -, 5 = +$. The integral involved reads

$$ZS' = - \int_{\Lambda/s}^{\Lambda} \frac{dk}{2\pi} \int_{-\infty}^{+\infty} \frac{d\omega}{2\pi} G_+(i\omega, k) G_-(i\omega - i\nu, k - q) u(-+ +-) u(-+ +-) \quad (\text{S57})$$

where q/ν is the net come-in momentum/frequency. If we assume they are zero, then

$$ZS' = -2u^2 \int_{\Lambda/s}^{\Lambda} \frac{dk}{2\pi} \int_{-\infty}^{+\infty} \frac{e^{i0^+\omega} d\omega}{2\pi} \frac{1}{i\omega - k^2} \frac{1}{i\omega + k^2} \quad (\text{S58})$$

Use the formula

$$\frac{1}{i\omega - k^2} \frac{1}{i\omega + k^2} = \frac{1}{2k^2} \left(\frac{1}{i\omega - k^2} - \frac{1}{i\omega + k^2} \right) \quad (\text{S59})$$

The first term does not contribute to the contour integral. Thus,

$$ZS' = 2u^2 \int_{\Lambda/s}^{\Lambda} \frac{dk}{2\pi} \int_{-\infty}^{+\infty} \frac{e^{i0^+\omega} d\omega}{2\pi} \frac{1}{2k^2} \frac{1}{i\omega + k^2} = u^2 \int_{\Lambda/s}^{\Lambda} \frac{dk}{2\pi} \frac{1}{k^2} = \frac{\Lambda^{-1}u^2}{2\pi} (s - 1)$$

Two come from $\pm k$. The result of this calculation does not depend on the regulator $e^{i0^+\omega}$. One would observe a weaker CDW instability. Namely,

$$\beta_{zs'}(u) = \Lambda \frac{du_{zs'}}{d\Lambda} = \frac{\Lambda^{-1}u^2}{2\pi} \quad (\text{S60})$$

- *BCS diagram.* Now consider the BCS contribution. We demand that the sub-indices part satisfies $\{5, 6\} = \{+, -\}$. There are two options. They contribute,

$$\begin{aligned} BCS &= -\frac{u^2}{2} \int_{\Lambda/s}^{\Lambda} \frac{dk}{2\pi} \int_{-\infty}^{+\infty} \frac{d\omega}{2\pi} G_+(i\omega, k) G_-(i\nu - i\omega, q - k) \\ &\quad - \frac{u^2}{2} \int_{\Lambda/s}^{\Lambda} \frac{dk}{2\pi} \int_{-\infty}^{+\infty} \frac{d\omega}{2\pi} G_-(i\omega, k) G_+(i\nu - i\omega, q - k) \end{aligned} \quad (\text{S61})$$

Still trace the zero input frequency and momentum,

$$BCS = \frac{u^2}{2} \int_{\Lambda/s}^{\Lambda} \frac{dk}{2\pi} \int_{-\infty}^{+\infty} \frac{d\omega}{2\pi} \left(\frac{1}{i\omega - k^2} \frac{1}{i\omega - k^2} + \frac{1}{i\omega + k^2} \frac{1}{i\omega + k^2} \right) \quad (\text{S62})$$

Note that the residue of $1/z^2$ is zero. Thus the BCS contribution is zero.

Both tree and one-loop contribute to β -function,

$$\frac{du}{dt} = u + \frac{\Lambda^{-1}u^2}{2\pi}, \quad (\text{S63})$$

which is Eq. 9 in the main text.